ISSN: 2754-4915

Journal of Material Sciences & Manufacturing Research

SCIENTIFIC Research and Community

Research Article

Open Access

Impact of Magnesium Oxide Nanoparticles on Hematological, Biochemical and Antioxidant Levels of Mrigal *Cirrhinus mrigala*

Vyshnav G, Sudhabose S and Rajan MR*

Department of Biology, The Gandhigram Rural Institute-Deemed to be University, Gandhigram, Tamil Nadu, India

ABSTRACT

Magnesium oxide nanoparticles were synthesized and characterized by using UV-Visible spectroscopy, SEM, XRD, EDAX, FTIR, and AAS. Toxicity tests were observed at 96 hours in different concentrations of magnesium oxide nanoparticles exposed in mrigal. The sub-lethal studies were conducted for 14 days. Biochemical and haematological parameters were estimated. The UV-Visible absorption spectra demonstrate that magnesium oxide nanoparticles were measured in the wavelength range of 200-1100. Morphological characteristics were observed by using SEM at the wavelength of 2µm. EDAX spectrum showed two peaks located between 0KeV to 10KeV. The peak at 1.2KeV comes from magnesium and the second peak at 0.3KeV indicates oxygen. XRD results confirmed the crystalline size of magnesium oxide nanoparticles and the approximate particle size is 10nm. The FT-IR spectrum was analysed at the wavenumber range of 400-4000cm-1and the functional groups are alcohols, alkaline, anhydride and sulfonate. Atomic absorption spectroscopies estimate the convergence of metallic components in magnesium oxide. Total protein and lipid content in the muscle, gill and liver of Mrigal is significantly increased and carbohydrate content decreased when reared in different magnesium oxide concentrations. All the blood parameters are gradually increased from lower concentration to higher concentration. In the DPPH assay, when hydrogen donating ability with the DPPH, the red colour turns to yellow colour. Hydroxyl radical scavenging assay showed that the polyunsaturated fatty acid moieties of cell damage in lower concentration compared to higher concentration.

***Corresponding author**

Rajan MR, Department of Biology, The Gandhigram Rural Institute-Deemed to be University, Gandhigram, Tamil Nadu, India.

Received: May 05, 2022; **Accepted:** May 18, 2023; **Published:** May 22, 2023

Keywords: Impact, MgO Nanoparticles, Biochemical, Haematological, Mrigal

Abbreviations

UV-Vis: UV-Visible spectroscopy
SEM: Scanning Electron Microscopy
EDAX: Energy Dispersive X-Ray Spectroscopy
XRD: X-Ray Diffraction
FT- IR: Fourier Transform Infrared Spectroscopy
AAS: Atomic Absorption Spectrophotometer
GNOC: Ground Nut Oil Cake
MgO: Magnesium Oxide
NPs: Nanoparticles
cu mm: Cubic Millimeter
g/dl: Grams Per Decilitre
N: Normality
µl: Microlitre
mEq/L: Milliequivalents Per Litre
H2O2: Hydrogen Peroxide
µmol: Micromoles
KBr: Potassium Bromide
θ: Theta
JCPDS: Joint Committee on Powder Diffraction Standards
KeV: Kiloelectron Volts
%: Percentage
±: Standard Deviation
LC50: Lethal Concentration 50
WBC: White Blood Corpuscle
RBC: Red Blood Corpuscle
nm: Nanometer
mg: Milligram.

Introduction

Nanotechnology is a sensationally new area in science, with viable applications in many sectors [1]. Nanotechnology is a novel and inventive instrument that has a wide range of purposes and huge capability in aquaculture and seafood safeguarding. It can give new advanced technologies for the management of drugs as freedom of antibodies and subsequently hold the confirmation for protecting cultivated fish against illness-causing microorganisms [2]. Nanoscience studies the phenomena and manipulation of materials at atomic, molecular and macromolecular scales and this field is of greatest interest to handling nanoparticles, nanostructured materials, nanoporous materials, nano pigments, nanotubes, nanoimprinting, quantum dots and so on [3]. Nanoparticles show novel characteristics such as large surface area, great activity, and high reactionary efficiency [4]. Nanoparticle involves in the detection of biological agents, illnesses, and harmful materials are a significant goal for biomedical diagnosis, criminological investigation, and environmental monitoring [5]. Among metallic nanoparticles, iron, iron oxide, selenium, zinc, copper, silver and magnesium oxide play a crucial role in aquaculture development [6]. Magnesium oxide nanoparticles (MgO NPs) have various advantages, compared to other metal nanoparticles, including minimal expense, non-toxic, biocompatible, stable under harsh processing conditions, significant biomedical applications

and strong antimicrobial activity without photo-activation [7]. MgO is a functional material with a wide range of use in various areas and has good bactericidal performance in aquatic environments [8]. Magnesium oxide is considered one of the most important compounds of magnesium and is used in various industries, including refractory materials, pharmaceuticals, waste remediation, glass manufacturing, and aquaculture. The symptoms of magnesium deficiency in fish are loss of appetite, poor growth, sluggishness, and convulsion followed by tetany. The biochemical characterization of organisms involves the determination of chemical properties like the quantity of carbohydrates, lipids, and proteins in tissues, gills, muscles, liver, etc. Biochemical parameters could be used as important and sensitive biomarkers in ecotoxicological studies concerning the effect of metal contamination and fish health [9]. MgO nanoparticles are acutely toxic to aquatic ecosystems because of its accumulation and extensive use, posing a severe threat to the environment [10]. The haematological indicators are important for evaluating the physiological state of a fish. A fish's physical changes depend upon species, age, sexual maturity, and health condition. DPPH assay (2, 2-diphenyl-1-picrylhydrazyl) was used to determine the radical scavenging properties of different extracts [11]. HRSA Hydroxyl radical is one of the potent reactive oxygen species. It responds with polyunsaturated fat moieties of cell layer phospholipids and damage to cells [12]. For the present study, Mrigal was utilized as the model organism, because it is a widely distributed Indian major carp that represents the majority of the total mass of the Indian sub-continent and its fishery is strongly dependent on the commercial and recreational demand [13]. The work related to the impact of magnesium oxide nanoparticles on the haematological, biochemical, and antioxidant levels of Mrigal *Cirrhinus mrigala* is scanty. Hence the present study was carried out.

Materials and Methods

Synthesis of Magnesium Nanoparticles

MgO nanoparticles are prepared by using $Mg(NO_3)_2$ $6H_2O$ and NaOH. In the beginning, 5.21g magnesium nitrate (0.2M) was dissolved in 200 ml distilled water into a breaker. 0.8g Sodium hydroxide(0.2 M) was dissolved in 200 ml of distilled water. 200 ml NaOH solution was added dropwise using a pipette kept under a magnetic stirrer for 3 hours. After 3 hours, the milky white colour precipitate formed, and the solution was kept under 2 hours for resting Centrifuged MgO gel for 15min by using water and ethanol. The pellet is spread on a plate in room temperature (28± 2° C) and dried for one full day. Grained the MgO NPs and keep them in a muffle furnace for 3 hours at 400°C.

Characterization of MgO Nanoparticles

UV-Visible spectroscopy (Thermoscientific Genesys 180 UV-Visible spectrophotometer) measures the extinction (scatter + absorption) of light passing through a sample. Nanoparticles have unique optical properties that are sensitive to the size, shape, concentration, agglomeration state and refractive index near the nanoparticle surface, which makes UV-Vis a valuable tool for identifying, characterizing, and studying nanomaterials. The most important factor of the technique is to give the information about the material when light falls on it. The morphology of the magnesium oxide nanoparticles was examined using SEM (VEGA3, TESCAN (Czech Republic) Model SEM). Crystalline size and arrangement of MgO nanoparticles determined by XRD (PANalytical/ X Pert3 Powder model of XRD). Energy Dispersive X-Ray Analysis (EDX), assigned as EDS or EDAX, is an x-beam procedure used to recognize the essential organization of materials. (BRUKER Nano, GmbH, D-12489). FTIR is a very versatile tool for the surface characterization of nanoparticles and provides a specific setup attached to the spectrometer (FT/IR – 4700 Model). MgO nanoparticle metallic properties were identified by using AAS. (Perkin Elmer A Analyst 100).

Mortality measures, like LC_{50} estimation, give a valuable method for assessing the poisonousness level of a particular minor component, and LC_{50} esteem was perceived as an adequate restricting centralization of contamination in water. Intense harmfulness bioassays (LC_{50}) are utilized to assess the poisonousness of heavy metals (MgO NPs) and evaluate the possibilities of different fish species to the harmful metals. Median lethal (LC_{50}) tests were carried out for 96 hrs by using probit analysis (Table 1). Based on the median lethal (LC_{50}) toxicity test, 1/100th (T1), $1/50^{th}$ (T2) and $1/10^{th}$ (T3) of median lethal value were selected as concentrations for sublethal (LD_{50}) test. The stock suspension was prepared as same as that of the acute toxicity test and fish were exposed for 14^{th} days.

Table 1: Estimation of the median lethal concentration of Magnesium oxide Nanoparticles on Mrigal

	Probability	95% Confidence Limits for concentration			95% Confidence Limits for log(concentration)[a]		
		Estimate	Lower Bound	Upper Bound	Estimate	Lower Bound	Upper Bound
LC1	0.01	2.536	2.168	6.128	343.267	147.086	1342100.931
LC5	0.05	2.330	2.048	4.982	213.774	111.789	95993.127
LC10	0.1	2.220	1.983	4.374	166.077	96.086	23646.295
LC15	0.15	2.146	1.937	3.965	140.066	86.420	9224.028
LC20	0.2	2.088	1.898	3.642	122.332	79.136	4381.513
LC25	0.25	2.037	1.864	3.366	108.918	73.069	2323.303
LC30	0.3	1.992	1.830	3.121	98.130	67.661	1321.178
LC35	0.35	1.950	1.796	2.897	89.089	62.567	788.591
LC40	0.4	1.910	1.760	2.689	81.282	57.502	488.201
LC45	0.45	1.871	1.717	2.494	74.381	52.166	311.839
LC5O	0.5	1.834	1.665	2.314	68.161	46.189	205.862

Biochemical characteristics such as Protein,carbohydrate,and lipid in gill, muscle and liver were estimated after 14 days exposure of to Mrigal [14-16].

Haematological parameters such as WBC, Polymorph Neutrophils, Lymphocytes, Eosinophils, Haemoglobin, RBC, Hematocrit (PCV), Platelet count, and Blood protein were estimated after the 14th day.

Antioxidant

DPPH assay (2, 2-diphenyl-1-picrylhydrazyl) was used to determine the radical scavenging properties of different extracts [11]. In the biological system, hydroxyl radical is one of the potent reactive oxygen species. It responds with polyunsaturated fat moieties of cell layer phospholipids and damage to cells [12].

Results

UV-Visible absorption spectroscopy is a widely used technique to examine the optical properties of the Nano sized particle. A range of wavelengths 200-1100 was used to measure the absorbance spectra of magnesium oxide nanoparticles. It exhibits a strong absorption band at 240nm as shown in Figure 1. The morphology, structure and size of the samples were investigated by SEM. Scanning Electron Microscope indicates that magnesium oxide nanoparticles are granular structures (Figure 2). According to the SEM images, the particle sizes of pure MgO nanocrystals ranged from 20-50 nm. The phase structure of chemically synthesized magnesium oxide nanoparticles is shown in Figure 3. The XRD diffraction peaks were 36.86° (111), 42.84° (200), 62.23° (220), 74.61° (311), and 78.59° (222). The structure and crystalline size of magnesium oxide nanoparticles were determined by XRD. The sample was scanned between angles 0° - 90° to obtain the equatorial reflection crystal size of magnesium oxide nanoparticles and was calculated by using the Scherer equation and approximate particle size 10nm.EDAX spectrum recorded on the magnesium oxide nanoparticles is shown as two peaks located between 0KeV to 10KeV (Figure 4). The maximum peak located on the spectrum at 1.2 KeV comes from magnesium. The second peak located on the spectrum at 0.3 KeV indicates oxygen. Magnesium is more abundant than oxygen (Table 1). The FT-IR measurement was carried out for identifying the possible chemical responsible for the reduction and capping of MgO synthesized. The FT-IR spectrum of magnesium oxide nanoparticles was analysed at the wavenumber range of 400-4000cm-1 (Figure 5). The spectra show bands at 3450, 2922, 1639, 1383, 1250, 810 and 674 cm-1 functional groups such as alcohol, phenol, alkaline, and ketone. The peaks observed at 810 cm-1 indicate the presence of magnesium oxide. Atomic absorption spectroscopy is used for estimating the convergence of metallic components in magnesium oxide. The concentration of magnesium oxide nanoparticles is directly proportional to the absorption of magnesium oxide nanoparticles (Figure 6).

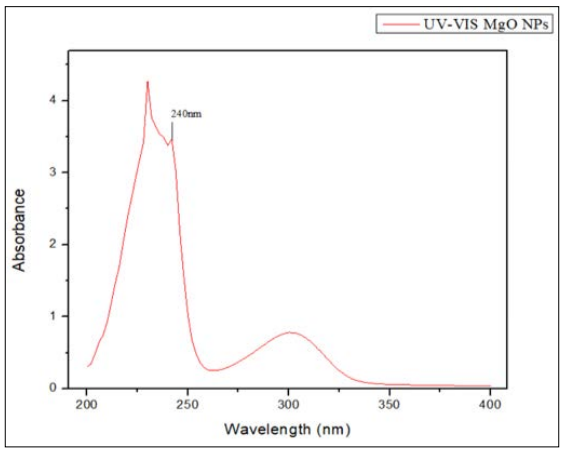

Figure 1: UV-VIS Spectroscopy analysis of magnesium oxide nanoparticles

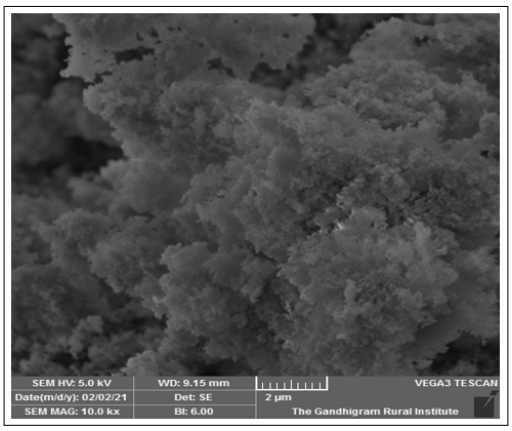

Figure 2: SEM image of Magnesium oxide nanoparticles

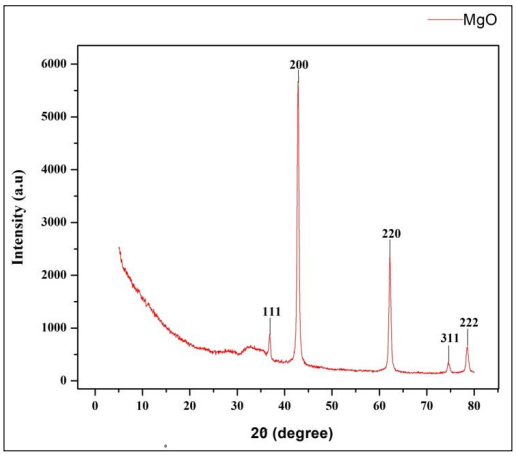

Figure 3: XRD image of Magnesium oxide nanoparticles

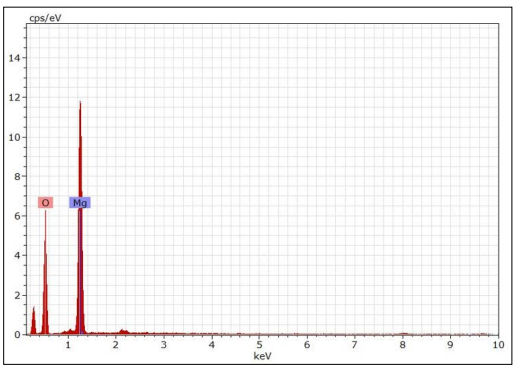

Figure 4: EDAX image of Magnesium oxide nanoparticles

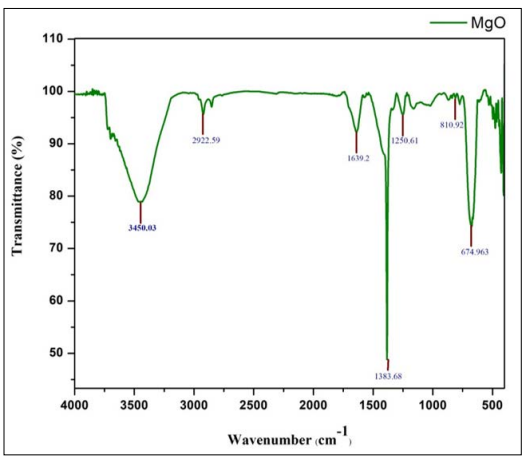

Figure 5: FTIR graph of Magnesium oxide nanoparticles

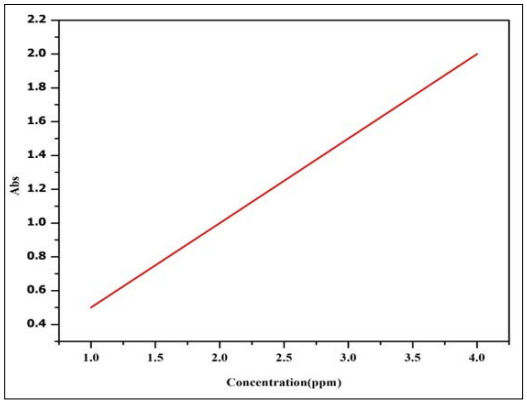

Figure 6: AAS graph of Magnesium oxide nanoparticles

Total protein content in the muscle, gill and liver of Mrigal is significantly increased when reared in different magnesium oxide concentrations. In lower concentrations protein is lower. Comparative to higher concentration protein is higher. Magnesium oxide is the cofactor of protein enzyme and its plays a vital role in the transporting of the same gill, muscle and liver (Figure 7). Total carbohydrate content in the muscle, gill and liver of Mrigal are higher in T0 and T1, T2, and T3 respectively lower in all concentrations because there is no feed for 14 days of the experiment (Figure 8). Total lipid content in the muscle, gill and liver of Mrigal is low in control compared to the higher concentration (Figure 9).

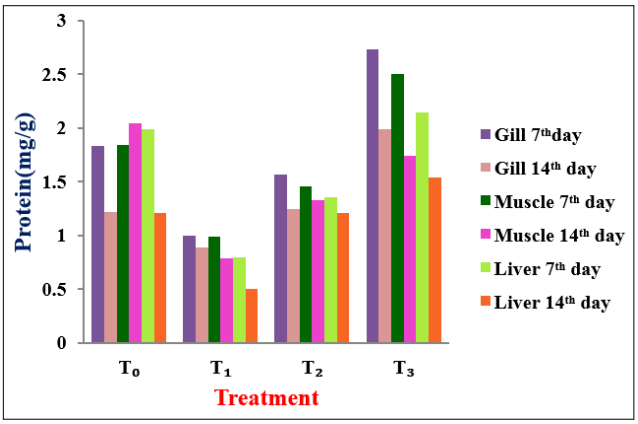

Figure 7: Total protein in gill, muscle and liver of Mrigal

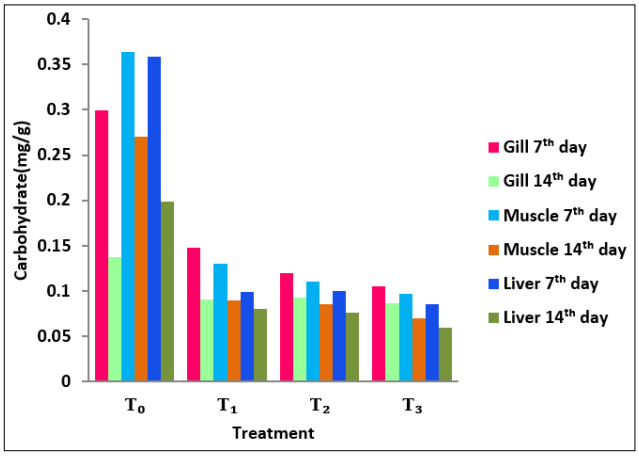

Figure 8: Total carbohydrates in gill, muscle and liver of Mrigal

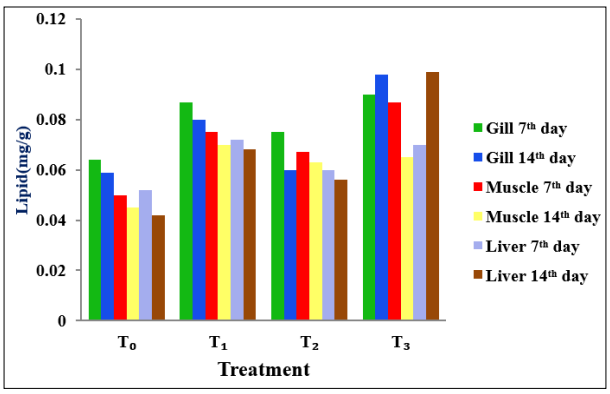

Figure 9: Total lipid in gill, muscle and liver of Mrigal

All blood parameters of Mrigal are gradually increased from lower concentration to higher concentration (Table 2).

Table 2: Haematological Parameters of Mrigal

Blood Parameters	Control T0	T1	T2	T3
RBC (Count) (Millions/cumm)	0.05	0.02	0.02	0.3
WBC (cells/cumm)	1,700	1,750	1,900	3,500
Haemoglobin (gm/Di)	0.7	0.6	0.9	1.2
Eosinophil (%)	0	0	1	1
Lymphocytes (%)	30	29	40	52
Neutrophils (%)	0.01	0.05	0.03	0.2
Haematocrit (%)	0.3	0.2	0.4	0.5
MCV	97	100	109	132
MCH	20	22	35	49
MCHC	21	23	38	52
Platelets count (cells/cumm)	26,000	27,000	29,000	35,000

Magnesium oxide is directly involved by increasing the activity of glutathione peroxidase (GPx), an important glutathione enzyme. Glutathione reacts with free radicals, especially toxic hydrogen peroxide when this enzyme is present. DPPH assay (2, 2-diphenyl-1-picrylhydrazyl) was used to determine the radical scavenging property. In this assay when hydrogen donating ability with the DPPH, The red colour turns to yellow colour present in the antioxidant. Higher concentration quickly reacted with the hydrogen donating ability compared to the lower concentration (Figure 10). Hydroxyl radical scavenging assay, hydroxyl radicals (which can damage cell membranes) like hydrogen peroxide is tested for their scavenging activity in the presence of different concentrations of the sample. In this study, HAS to react with the polyunsaturated fatty acid moieties of cell damage in lower concentrations compared to higher concentrations (Figure 11).

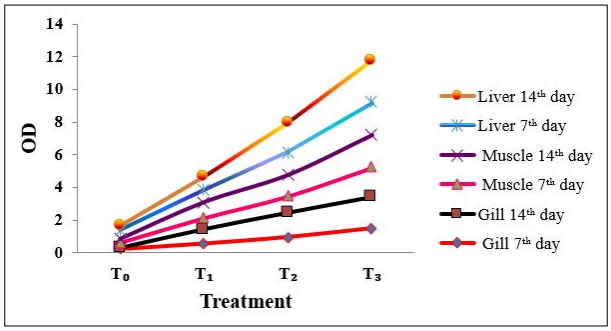

Figure 10: DPPH Assay (2, 2-Diphenyl-1-Picrylhydrazyl) on gill, muscle and liver of Mrigal

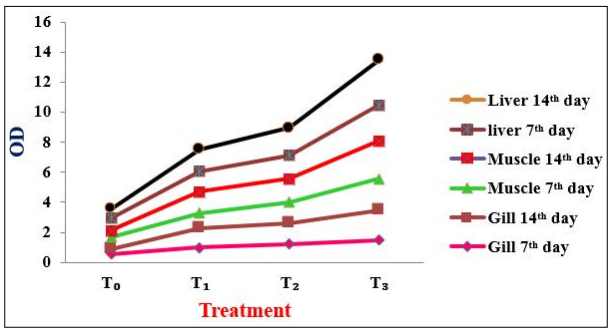

Figure 11: Hydroxyl Radical scavenging activity

Discussion

The UV–Vis spectroscopy technique is a reliable and helpful tool for identifying synthesized nanomaterials at a primary level. A range of wavelengths 200-1100 was used to measure the absorbance spectra of magnesium oxide nanoparticles. It exhibits a strong absorption band at 240nm. Jeevanandam et al., reported that the MgO nanoparticles are prepared via *Amaranthus tricolour* leaf extract and the optical absorbance of those nanosized particles is observed in the UV region 320 nm [17]. The UV-visible spectra of the prepared MgO nanopowder in the absorbance mode, and in the wavelength range between 200–900 nm to determine the absorbance of MgO NPs obtained a distinctive absorption band of MgO up to 800 nm [18]. The UV-Visible spectroscopy was adjusted to distinguish the age of Magnesium oxide nanoparticles [19]. Scanning Electron Microscope indicates that magnesium oxide nanoparticles are clumped structure and were observed in 200nm to 500nm. The scanning electron microscope (SEM) of the MgO particles shows a unique crystalline structure and the SEM also shows the size ranging from 200 to 300 nm [20]. Fedorov et al., reported that during magnesium hydroxide calcination at 730° and oxide formation, the platelike shape of the particles persists, even though it is a nonequilibrium shape for MgO [21]. The formation of interfused $Mg(OH)_2$ nanoflakes and coral-like hierarchical MgO nanostructure made up of stacked nanoflakes [22]. Scanning Electron microscopic images of MgO nanoparticles show magnification at 300, 500 and 700° depicts that the nanoparticles are appearing as discrete particles [23]. Sellik et al., reported that monocrystalline material and randomly aggregated nanoparticles were visible [24]. There were fewer aggregate particles with MgO-1 than with MgO-2. MgO-1 particles show sheet structure and MgO-2 particles were elongated. Jo-Yong Park reported that the normal molecule size of the MgO NPs fell in the range from 20 to 50 nm, depending upon the strategy used to wash $Mg(OH)_2$ [25]. Janet Priscilla reported that combustion-derived product shows high porosity, foam, and fluffy nature [26]. Observations have shown that all synthesized nanomaterials are spherical and agglomerated. The XRD results revealed the crystalline structure of magnesium oxide nanoparticles. The XRD diffraction peaks 36.86° (111), 42.84° (200), 62.23° (220), 74.61° (311), and 78.59° (222) were observed. Kalaimathi et al., reported that X-ray diffraction patterns of the synthesized magnesium oxide nanoparticles show strong diffraction peaks(2Θ°) at 32.79, 36.83, 50.58, 58.53, 61.89, 67.84 and 71.87 corresponds to(joint committee on powder diffraction standards-JCPDS No. 36-1451) 111, 200, 220, 221, 311, 222, and 321 lattice planes [27]. The XRD measurements revealed a typical single crystalline periclase phase of bulk MgO [28]. Anil Kumar et al., reported that the X-ray diffraction peaks of the samples at 2θ, 36.58° (1 1 1), 42.63° (2 0 0), 62° (2 2 0), well matched with space group fm-3m (225) and JCPDS card No. 78-0430. EDAX spectrum recorded on the magnesium oxide nanoparticles is shown as two peaks located between 0KeV to 10KeV. The EDAX indicates the purity of the synthesized MgO NPs and it has two peaks the first peak is magnesium and the second peak indicates oxygen. Rajendran et al., reported that the NPs consist of Mg, Cu and O which confirms the substitution of Cu in MgO [29]. In the doped samples, the concentration of Cu is found to be 06.19%. In the Pure MgO NPs, the chemical compositions of Mg and O are found to be 56.61% and 43.39% respectively. The peaks correspond to Mg and O elements with an average atomic percentage ratio of 58:42 [25]. The EDAX spectrum shows that the product was principally composed of Mg and O, and their respective atomic content [30]. FT-IR spectrum of magnesium oxide nanoparticles was analysed at the wavenumber range of 400-4000cm^{-1}. The FT-IR spectrum of magnesium oxide nanoparticles shows bands at 3450, 2922, 1639, 1383, 1250, 810 and 674 cm^{-1} correspond to functional groups such as alcohol, phenol, alkaline, and ketone. The peaks observed at 810 cm^{-1} indicate the presence of magnesium oxide. Balamurugan et al., reported that MgO NPs using the FTIR spectroscopy and found the vibration mode in the range 487-677 cm^{-1} wavenumber, indicating the Mg-O-Mg bonds [31]. Mohammad Moslem Imani and Mohsen Safaei reported that the peaks observed below 850cm^{-1} confirmed the magnesium oxide [32]. The MgO NPs used the FTIR and found the peak ~ 3702 cm^{-1} revealing the presence of a hydroxyl group and the broadband at 473 cm^{-1} indicating the Mg-O vibration [33].

Atomic absorption spectroscopy is used for estimating the convergence of metallic components in magnesium oxide. The concentration of magnesium oxide nanoparticles is directly proportional to the absorption of magnesium oxide nanoparticles. Ben Haha et al., reported the effect of high inherent MgO content on AAS and found that for water glass-activated slag paste, the compressive strength at 28 days increased by 50– 80% with increasing MgO content from 8% to 13% [34]. The heavy metals were detected by atomic absorption spectroscopy according to the absorption of light by free metallic ions. The major common heavy metals such as Cr, Co, Pb, Cd, and Ni in tanning wastewater including were measured before and after MgO-NPs treatment using atomic adsorption spectroscopy [35]. The concentration of magnesium oxide nanoparticles is directly proportional to the absorption of magnesium oxide nanoparticles.

The mortality/survival of Mrigal in control and magnesium oxide-treated tanks was recorded after 96 hours and the concentration at which 50% mortality of fish occurred was taken as the median lethal concentration (LC_{50}). The toxicity of the MgO NPs with different mammalian cell lines at a concentration range of ≥ 323.39 µg/mL as LC_{50} [36]. The sub-lethal concentration of magnesium oxide nanoparticles such as control, 1/10, 1/50 and 1/100 and different concentration of magnesium oxide nanoparticles was exposed for 14 days. John Thomas et al., reported that MgO-n

whereas in the bulk at 50,100, 150 and 200ppm there was 33%, 35%, 66% and 66% mortality respectively at 120hrs in Tilapia [37]. Gavit and Patil reported that LC_{50} values were found to be 1762 ppm, 1509 ppm, 1281 ppm and 1117 ppm at 24, 48, 72 and 96 hours respectively [38].

Biochemical characterization such as protein, carbohydrates and lipids in Mrigal are higher in T3, and T2 compare to the control. Carbohydrate at T3, and T2 is lower than when compared to T1 and control. Palanisamy et al., reported that concentration-based increase and decrease in protein, lipids and carbohydrates [39]. The Cu, Zn, Fe, Ca, Mg, Na and K, has improved the synthesis of protein in aquatic animals and the optimum concentration of Mg can improve the synthesis of protein in shrimps and fishes [40]. The attributed to the increase in lipid metabolism as Mg plays a critical role in the normal metabolism of lipids as a cofactor in a large number of enzymatic and metabolic reactions [41]. The concentration-based increase and decrease of protein, carbohydrate and lipid. The lipid content in magnesium oxide nanoparticles exposed to Common carp is increased when the concentration is increased [42].

All the blood parameters of Mrigal are gradually increased from lower concentration to higher concentration. Haematological parameters are very helpful in the judgement of the health condition of fish species. The complete blood count of Mrigal progressively increased from lower concentration to higher concentration. Nafiseh Muzaheri et al., reported that toxicity assessment of standard haematological parameters, including determination of white blood cells (WBC), red blood cells (RBC), hematocrit (HCT), platelet count (PLT), haemoglobin (Hb) levels, mean corpuscular haemoglobin (MCH), mean corpuscular haemoglobin concentration (MCHC) and mean corpuscular volume (MCV) was observed that white blood cells significantly increase at MgO nanoparticles doses of 250 and 500 ug/ml respectively ($P < 0.05$) [43]. Milad Adel et al., reported that the nominal concentration of 0.0026 mgL1 showed a significant decrease (p50.05) in Ht and lymphocyte count after 10, 20 and 30 days of exposure compared to the control [44]. Caspian brown trout showed a significant decrease (p50.05) of RBC, and Hb and an increase (p0.05) of neutrophile and leukocyte count after 20 and 30 days of exposure compared to the control. Veeran Srinivasan et al., reported that the increase in total haemocyte count (THC) and different haemocyte count (DHC) (hyalinocytes, semi granulocytes and granulocytes) recorded in the test prawns suggests that MgO NPs have influenced the production of haemocytes to maintain good health [45]. Similarly, optimum levels of dietary Mg, nano-Zn, Cu, Fe and Mn have also produced better values on total haemocyte count and different haemocyte counts in M.rosenbergii PL and L. japonicas. DPPH assay (2, 2-diphenyl-1-picrylhydrazyl) when hydrogen donating ability with the DPPH, The red colour turns to yellow colour present in the antioxidant. Higher concentration quickly reacted with the hydrogen donating ability compared to the lower concentration. The MgO nanoparticles come into contact with sufficient oxygen in the bacterial cell wall, they tend to generate superoxides. The super oxides formed are highly reactive in free-radical DPPH interacts with an odd electron, the greatest absorption takes place at 517 nm (purple colour). A free-radical scavenger antioxidant reacts to DPPH to form DPPH-H, which has a lower absorbance than DPPH because of the lower amount of hydrogen. In comparison to the DPPH-H state, this radical version causes decolourization [46]. In vitro, antioxidant activity of MgO NPs by DPPH and reducing power assay has proved that biologically synthesized MgO NPs have 65 % inhibition activity. The potential antioxidant activity of biologically synthesized MgONPs may be due to the presence of bioactive components of the plant extract. Hence, the biologically synthesized MgO NPs have potential in vitro antioxidant activity [47].

Hydroxyl radical scavenging assay found to damage body cells. HAS to react with the polyunsaturated fatty acid moieties of cell damage in lower concentrations compared to higher concentrations. (Deeptha Rajaram and Nazeer, reported that the hydroxyl radical scavenging activity of the sample was determined by the methods of Rosen [48]. The hydroxyl radicals are generated in a Fenton reaction and were visualized by an ESR spectrometer. The ESR signal is inhibited by the presence of antioxidants, which compete with 5,5-dimethylpyrroline N-oxide (DMPO) for hydroxyl radicals. Hydroxyl radical scavenging ability was calculated with the following equation, in which H and H0 are relative peak heights of radical signals with and without the sample, respectively [49].

Conclusion

Magnesium oxide nanoparticles were synthesized and characterised by using UV-Visible spectroscopy, SEM, XRD, EDAX, FTIR, and AAS. All the haematological parameters of Mrigal increased with an increased quantity of MgO nanoparticles. Total protein and lipid content in the muscle, gill and liver of Mrigal is significantly increased and carbohydrate content decreased when reared in different magnesium oxide concentrations. In vitro, the antioxidant activity of MgO NPs by DPPH and reducing power assay has proved that biologically synthesized MgO NPs have 65 % inhibition activity. HAS to react with the polyunsaturated fatty acid moieties of cell damage in lower concentrations compared to higher concentration

Conflict of Interest: The authors declare no conflict of interest.

Authors Contribution

G. Vyshnav: Laboratory experiments were conducted starting from the collection of fish, haematological, biochemical and antioxidant levels of Mrigal Cirrhinus mrigala S. Sudhabose: Done experiments related to the synthesis of magnesium oxide nanoparticles and characterization using UV- Vis, SEM, EDAX, XRD, and FT-IR, M.R. Rajan: The research work was formulated and guidance was given to the first and second authors for execution.

Acknowledgement: The authors thank the Department of Biology, The Gandhigram Rural Institute- Deemed to be University, Dindigul, Tamil Nadu, India for giving laboratory facilities.

References

1. Rajive Saini, Saini S, Sharma S (2010) Nanotechnology: the future medicine. J Cut Aaesth Sur 3: 32-33.
2. Sameh Nasr-Eldahan, Nabil-Adam A, Shreadah MA, Maher AM, El-Sayed Ali T (2021) A review article on nanotechnology in aquaculture sustainability as a novel tool in fish disease control. Aqua Int 29: 1459-1480.
3. Lijie Zhang, Webster TJ (2009) Nanotechnology and nanomaterials: promises for improved tissue regeneration. Nano today 4: 66-80.
4. Miklos M, Pelyhe C (2013) Myths and facts about the effects of nano selenium in farm animals-mini-review. Eur Chem Bull 2: 1049-1052.
5. Mrinmoy De, Ghosh PS, Rotello VM (2008) Applications of nanoparticles in biology. Adv Mat 20: 4225-4241.
6. Fasil Dawit, Moges, Patel P, Parashar SKS, Das B (2019) Mechanistic insights into diverse nano-based strategies for

aquaculture enhancement: A holistic review. Aqua 519: 734770.

7. Marwa, Abdel-Aziz, Emam TM, Elsherbiny EA (2020) Bioactivity of magnesium oxide nanoparticles synthesized from cell filtrate of endobacterium Burkholderia rinojensis against Fusarium oxysporum. Mat Sci and Engin C 109: 110617.
8. Sachindri, Rana, Kalaichelvan PT (2011) Antibacterial activities of metal nanoparticles. Antibacterial Activities of Metal Nanopart 11: 21-23.
9. Öner M, Atli G, Canli M (2008) Changes in serum biochemical parameters of freshwater fish Oreochromis niloticus following prolonged metal (Ag, Cd, Cr, Cu, Zn) exposures. Environ Toxi Chem: An Int Journal 27: 360-366.
10. Suresh Bibi, Khan S, Taimur N, Daud MK, Azizullah A (2019) Responses of morphological, physiological, and biochemical characteristics of maize (Zea mays L.) seedlings to atrazine stress. Environ Monit Assess 191: 1-14.
11. Chang ST, Wu JH, Wang SY, Kang PL, Yang NS, et al. (2001) Antioxidant activity of extracts from Acacia confusa bark and heartwood. J Agricult Food Chem 49: 3420-3424.
12. 12. Halliwell B, utteridge JM (1981) Formation of a thiobarbituric-acid-reactive substance from deoxyribose in the presence of iron salts: the role of superoxide and hydroxyl radicals. FEBS letters 128: 347-352.
13. Velmurugan B, Selvanayagam,M, Cengiz EI, Unlu E (2007) Histopathology of lambda-cyhalothrin on tissues (gill, kidney, liver and intestine) of Cirrhinus mrigala. Enviro Toxi Pharma 24: 286-291.
14. Lowry OH, Rosenbrough NJ, Farr AL (1951) Protein measurement with the Folin Phenol Reagent. J Biol Chem 193: 265-275.
15. Carrol NV, Longley RW, Roe JH (1956) Glycogen determination in liver and muscle by use of anthrone reagent. J Biol Chem 220: 583-593.
16. Folch J, Lees M, Stanley SGH (1957) A simple method for the isolation and purification of total lipids from animal tissues. J of Biochem 226: 497-509.
17. Jeevanandam J, San Chan Y, Wong YJ, Hii YS (2020) Biogenic synthesis of magnesium oxide nanoparticles using Aloe barbadensis leaf latex extract. In IOP Conference Series: Materials Science and Engineering 943: 012030.
18. Almontasser A, Parveen A, Azam A (2019) Synthesis, Characterization and antibacterial activity of Magnesium Oxide (MgO) nanoparticles. In IOP Conference Series: Mat Sci Eng 577: 012051.
19. Rahul Patil, Chougale AD (2021) Analytical methods for the identification and characterization of silver nanoparticles: A brief review. Mat Today Proc 47: 5520-5532.
20. Veera Boddu M, Viswanath DS, Maloney SW (2008) Synthesis and characterization of coralline magnesium oxide nanoparticles. J Amer Cera Soc 91: 1718-1720.
21. Fedorov PP, Tkachenko EA, Kuznetsov SV, Voronov VV, Lavrishchev SV (2007) Preparation of MgO nanoparticles. Inorg Mat 43: 502-504.
22. Mageshwari K, Sathyamoorthy R (2012) Studies on photocatalytic performance of MgO nanoparticles prepared by wet chemical method. Trans Ind Inst Metals 65: 49-55.
23. Sundrarajan M, Suresh J, Gandhi RR (2012) A comparative study on antibacterial properties of MgO nanoparticles prepared under different calcination temperature. Digest J Nanomat and biostr 7: 983-989.
24. Sellik A, Pollet T, Ouvry L, Briançon S, Fessi H, et al. (2017) Degradation of paraoxon (VX chemical agent simulant) and bacteria by magnesium oxide depends on the crystalline structure of magnesium oxide. Chemico-Biol Inter 267: 67-73.
25. Jo-Yong, Park Y, Lee YJ, Jun KW, Baeg JO, et al. (2006) Chemical synthesis and characterization of highly oil dispersed MgO nanoparticles. J Ind Engin chem 12: 882-887.
26. Janet Priscilla J, Daniel R, Gayathri S, Melcita A, et al. (2017) Solution Combustion Mediated Synthesis and Characterization Of Magnesium Oxide Nanoparticles.. International Research Journal of Engineering and Technology (IRJET) 04: 405-408.
27. Kalaimathi M, Hariharan K, Vishnu S, Chinnasamy R (2021) Parallel synthesis and optimization of magnesium oxide nanoparticles using Tridax procumbens and Myristica fragrance. Curr Res in Green and Sust Chem 4: 1-5.
28. Rizwan, Wahab, Ansari SG, Dar MA, Kim YS, Shin HS (2007) Synthesis of magnesium oxide nanoparticles by sol-gel process. In Mat Sci Forum 558: 983-986.
29. Anil Kumar M, Mahendra B, Nagaswarupa HP, Surendra BS, Ravikumar CR, et al. (2018) Photocatalytic studies of MgO nanopowder; synthesized by the green mediated route. Mat Today: Proceedings 5: 22221-22228.
30. Rajendran V, Deepa B, Mekala R (2018) Studies on structural, morphological, optical and antibacterial activity of Pure and Cu-doped MgO nanoparticles synthesized by co-precipitation method. Mat Today: Proc 5: 8796-8803.
31. Umaralikhan L, Jamal Mohamed Jaffar M (2018) Green synthesis of MgO nanoparticles and it antibacterial activity. Iran J Sci Tech, Transactions A: Sci 42: 477-485.
32. Balamurugan S, Ashna L, Parthiban P (2014) Synthesis of nanocrystalline MgO particles by combustion followed by annealing method using hexamine as a fuel. J Nanotech 1: 1-6.
33. Mohammad Moslem Imani, Safaei M (2019) Optimized synthesis of magnesium oxide nanoparticles as bactericidal agents. J Nanotech 1: 1-6.
34. Selvam NCS, Kumar RT, Kennedy LJ, Vijaya JJ (2011) Comparative study of microwave and conventional methods for the preparation and optical properties of novel MgO-micro and nano-structures. J Alloys and Compounds 509: 9809-9815.
35. Ben Haha M, Lothenbach B, Le Saout GL, Winnefeld F (2011) Influence of slag chemistry on the hydration of alkali-activated blast-furnace slag-Part I: Effect of MgO. Cement and Concrete Research 41: 955-963.
36. Amr Fouda, Awad MA, Eid AM, Saied E (2021) An Eco-Friendly Approach to the Control of Pathogenic Microbes and Anopheles stephensi Malarial Vector Using Magnesium Oxide Nanoparticles (Mg-NPs) Fabricated by Penicillium chrysogenum. Int J Molecul Sci 22: 5096.
37. Suresh Verma K, Nisha K, Panda PK, Patel P, Kumari P (2020) Green synthesized MgO nanoparticles infer biocompatibility by reducing in vivo molecular nanotoxicity in embryonic zebrafish through arginine interaction elicited apoptosis. Sci of Total Enviro 713: 136521.
38. John Thomas, Thanigaivel S, Vijayakumar S, Acharya K, Shinge D, et al. (2014) Pathogenecity of Pseudomonas aeruginosa in Oreochromis mossambicus and treatment using lime oil nanoemulsion. Colloids and Surfaces B: Biointerf 116: 372-377.
39. Gavit PJ, Patil RD (2016) Acute toxic effects of acephate on freshwater fish Puntius sophore (Hamilton). J Ent Zoo Stu 4: 1364-1366.
40. Palanisamy PG, Sasikala D, Mallikaraj NB, Natarajan GM (2011) Electroplating industrial effluent chromium induced changes in carbohydrates metabolism in air-breathing catfish Mystus cavasius (Ham). Asian J Exp Biol Sci 2: 521-524.
41. Veeran Srinivasan, Bhavan PS, Rajkumar G, Satgurunathan T,

Muralisankar T (2017) Dietary supplementation of magnesium oxide (MgO) nanoparticles for better survival and growth of the freshwater prawn Macrobrachium rosenbergii post-larvae. Biol Tra Ele Res 177: 196-208.

42. Lall SP (2002) The minerals In: Halver JE and Hardy DV(Eds) Fish Nutrition 3 edn. Acad. Press Inc San Diego pp: 259-308.
43. Kevasasus, Palanisamy PG, Sasikala D, Mallikaraj NB, Natrajan GM (2011) Electroplating industrial effluent chromium induced changes in carbohydrates, metabolism in air breathing cat fish Mystus cavasius. Asian J Exper Biol Sci 2: 521-524.
44. Nafiseh Muzaheri, Naghsh N, Karimi A, Salavati H (2019) In vivo toxicity investigation of magnesium oxide nanoparticles in rat for environmental and biomedical applications. Iran J biotech 17: 1-5.
45. Milad Adel, Yeganeh S, Dadar M, Sakai M, Dawood, MA (2016) Effects of dietary Spirulina platensis on growth performance, humoral and mucosal immune responses and disease resistance in juvenile great sturgeon (Huso huso Linnaeus, 1754). Fish & Shellfish Immunology 56: 436-444.
46. Siddartha Baliyan, Mukherjee R, Priyadarshini A, Vibhuti A, Gupta A, et al. (2022) Determination of Antioxidants by DPPH Radical Scavenging Activity and Quantitative Phytochemical Analysis of Ficus religiosa. Mole 27: 1326.
47. John Sushma N, Prathyusha D, Swathi G, Madhavi T, Deva Prasad Raju B, et al. (2016) Facile approach to synthesize magnesium oxide nanoparticles by using Clitoria ternatea-characterization and in vitro antioxidant studies. Applied Nanoscience 6: 437-444.
48. Deeptha Rajaram, Nazeer RA (2010) Antioxidant properties of protein hydrolysates obtained from marine fishes Lepturacanthus savala and Sphyraena barracuda. Int J Biotech Biochem 6: 435-445.
49. Sampath Kumar NS, Nazeer RA, Jaiganesh R (2012) Purification and identification of antioxidant peptides from the skin protein hydrolysate of two marine fishes, horse mackerel (Magalaspis cordyla) and croaker (Otolithes ruber). Amino Acids 42: 1641-1649.